Available online at www.sciencedirect.com
SCIENCE DIRECT®
Polymer 44 (2003) 4791–4803
polymer
www.elsevier.com/locate/polymer

Rates and product properties of polyethylene produced by copolymerization of 1-hexene and ethylene in the gas phase with $(n\text{-BuCp})_2ZrCl_2$ on supports with different pore sizes

P. Kumkaew[a,b], L. Wu[a], P. Praserthdam[b], S.E. Wanke[a,*]

[a]*Department of Chemical and Materials Engineering, University of Alberta, Edmonton, Alberta, Canada T6G 2G6*
[b]*Department of Chemical Engineering, Chulalongkorn University, Bangkok 10300, Thailand*

Received 4 February 2003; received in revised form 25 April 2003; accepted 28 May 2003

Abstract

The effects of catalyst support pore size and reaction conditions ($T = 40–100$ °C; ethylene pressure = 1.4 MPa; 1-hexene concentration = 0–47 mol/m^3) on gas-phase polymerization rates and product properties were studied. Catalysts were prepared by impregnation of mesoporous molecular sieves (pore sizes of 2.5–20 nm) with methylaluminoxane and $(n\text{-BuCp})_2ZrCl_2$. Temperature rising elution fractionation, differential scanning calorimetry and size exclusion chromatography were used to characterize the products. The results showed that these catalysts contained multiple types of catalytic sites and that the types of sites were a strong function of the support pore size. Ethylene polymerization and 1-hexene incorporation rates were strong functions of support pore size, 1-hexene concentration, and temperature. Large-pored catalysts had higher 1-hexene incorporation rates and the rate of 1-hexene incorporation was a function of polymerization time. Highest polymerization rates were obtained at 80 °C and 1-hexene concentration of 4–12 mol/m^3; high 1-hexene concentrations resulted in large decreases in polymerization rates.

Keywords: Gas-phase ethylene polymerization; Supported metallocene catalysts; TREF and DSC characterization

1. Introduction

Metallocene catalysts are frequently referred to as single-site catalysts because the polymers produced with these catalysts frequently have narrow molar mass distributions, i.e. polydispersities close to 2 [1,2]. However, temperature rising elution fractionation (TREF) results of Soga et al. [3] with ethylene/1-hexene copolymers produced by homogeneous Cp_2ZrCl_2–methylaluminoxane (MAO) catalysts suggested that these catalyst systems contained two different types of catalytic species. Estrada and Hamielec [4] proposed a two-site model for ethylene homopolymerization with homogeneous Cp_2ZrCl_2–MAO catalyst based on activity profiles and size exclusion chromatography (SEC) results. Subsequently, Wang et al. [5] made similar observations for homogeneous Cp_2ZrCl_2–MAO and Cp_2ZrCl_2–butylaluminoxane (BAO) catalysts; they proposed a two-site model for Cp_2ZrCl_2–MAO and a three-site model for Cp_2ZrCl_2–BAO. Crystallization analysis fractionation (CRYSTAF) results of Kim and Soares [6] with ethylene/1-hexene copolymers produced during slurry operation with various silica supported metallocenes led to the conclusion that these supported catalysts contained two or more types of catalytic sites. We recently reported that the pore size of supports has a significant effect on the gas-phase polymerization rates for ethylene homopolymerization and ethylene/1-hexene copolymerization over supported $(n\text{-BuCp})_2ZrCl_2$–MAO catalysts [7]. Similar effects of support pore size on activity during slurry polymerizations using supported Cp_2ZrCl_2–MAO catalysts have also been reported by Sano and co-workers [8–11]. This effect of pore size on catalytic activity suggests that pore size influences the nature of the catalytic sites for supported zirconocene catalysts.

In the current work, the properties of polyethylenes produced in the gas phase with $(n\text{-BuCp})_2ZrCl_2$–MAO on supports with different pore sizes are presented. TREF, SEC and differential scanning calorimetry (DSC) were used for

* Corresponding author. +1-780-492-3817; fax: +1-780-492-2881.
E-mail address: sieg.wanke@ualberta.ca (S.E. Wanke).

0032-3861/03/$ - see front matter © 2003 Elsevier Science Ltd. All rights reserved.
doi:10.1016/S0032-3861(03)00473-7

characterization of the products. The effects of temperature and 1-hexene concentration on properties and activities are presented. Polymerization was carried out in the gas phase because gas-phase polymerization is widely used commercially for the production of linear low density polyethylene (LLDPE). TREF, DSC and SEC characterization of polyethylenes produced with metallocene catalysts in slurry reactors have been reported by others [3–7,12,13]. However, no such studies for polyethylenes produced with metallocene catalyst in gas-phase reactors have been reported, even though it has been predicted that gas-phase processes will be used for commercial production of LLDPE with metallocene catalysts [14]. Very little information is available about the effects of reaction temperature and comonomer concentration on the rate of polymerization and comonomer incorporation during gas-phase polymerization with supported metallocene catalysts; results on these topics are presented below.

2. Experimental

2.1. Materials

The catalysts used are described in Table 1; the numbers in the catalyst designation, e.g. the 2.6 in CAT2.6, indicate the pore diameter of the support, in nm, used to make the catalyst. A simple impregnation procedure, consisting of the addition of MAO to the dehydrated support followed by the addition of $(n\text{-BuCp})_2ZrCl_2$ to the MAO treated support, was used for the preparation of all of the catalysts. The compositions of the catalysts given in Table 1 were calculated from the amounts and compositions of the materials used in the impregnation. All the support, MAO and $(n\text{-BuCp})_2ZrCl_2$ used in a preparation ended up in the final catalyst because only the toluene was removed by evacuation. Hence, the overall composition of the catalyst is known, but the spatial distribution of the components in the catalysts are not known. Detailed preparation procedures for the catalysts and the supports for these catalysts, except for the support used for CAT2.5, have been presented previously [7]. The support for CAT2.5 was prepared by mixing 100 g of an aqueous solution of cetyltrimethylammonium (CTMA) hydroxide, made from a 25 mass% aqueous CTMA chloride solution, with 54 g of a 15 mass% tetramethylammonium silicate aqueous solution and the addition of 39.5 g of LUDOX® HS-40 colloidal silica. The mixture was kept for 16 h in a sealed reactor at 80 °C and at 95 °C for an additional 72 h. The solid product was filtered, air dried and treated in flowing nitrogen at 540 °C for 1 h and in flowing air at 540 °C for 6 h. The resulting product had a very narrow pore size distribution with an average pore diameter of 2.5 nm. All the materials used in the preparation of the support for CAT2.5 were obtained from Aldrich. All other materials used in this study have been described previously [7].

2.2. Polymerization procedure

The previously described 1-L stainless steel reactor [7,15] was used for all the polymerization experiments. The reactor was operated in the semi-batch mode with ethylene addition at rates necessary to maintain constant reactor pressure. The desired amount of 1-hexene was injected into the reactor at the beginning of each run prior to the injection of the catalyst. The 1-hexene was all added at the beginning of each run. Neat tri-isobutyl aluminum (TIBA) was also injected into the reactor prior to the injection of the solid catalyst. The solid catalyst was injected into the reactor using high-pressure ethylene. Additional details of the polymerization procedure have been presented by Kumkaew et al. [7].

2.3. Characterization methods

TREF was used to obtain information on the branching structure of the polymer. The analytic TREF procedure consisted of an off-column crystallization step in which the PE was dissolved in *o*-xylene at 125 °C (1 mg PE/ml *o*-xylene) followed by cooling of the polymer solution at 1.5 °C/h to −8 °C. During the cooling the PE crystallized onto glass beads (80–100 mesh). The crystallized sample was filtered into a TREF column (9.5 mm in inside diameter and 63.5 mm in length), which contained similar sized glass

Table 1
Description of catalysts

Catalysts	Support properties			Zr content mass%	Al/Zr ratio
	Pore diameter, nm	Pore volume, cm^3/g	Surface area, m^2/g		
CAT0.54[a]	0.54	–	435	0.33	170
CAT2.5	2.5	0.6	889	0.33	170
CAT2.6	2.6	1.3	1130	0.38	150
CAT5.8	5.8	0.8	980	0.34	170
CAT7.2	7.2	1.1	870	0.33	170
CAT15	15	1.3	330	0.34	170
CAT20	20	1.6	310	0.34	170

[a] silicalite used as support.

beads. The column was placed into the elution compartment of the custom-built TREF apparatus, and PE was eluted from the column by flowing *o*-dichlorobenzene (1.0 ml/min) by heating the column from 0 to 125 °C at a constant rate of 1.0 °C/min. The concentration of eluted PE was measured with an on-line IR detector tuned to 2860 cm^{-1}. Linear paraffins (C_{40} and C_{60}), linear polyethylene reference materials (1475, 1482, 1483 and 1484 from NIST) and 17 linear polyethylene samples prepared in our laboratory by preparative TREF (polydispersities <1.3 and number average molar masses, M_N, of 1000–10,000) were used to obtain a correlation between TREF elution temperature, T, and methyl group concentration $[CH_3]_T$. The obtained correlation, with T in °C, is

$$[CH_3]_T = \frac{CH_3 \text{ groups}}{1000 \text{ Carbons}} = 76.37 - 1.20T + 0.0044T^2 \quad (1)$$

Additional details on the TREF procedure have been presented previously by Huang et al. [16] and Zhang et al. [17]. The above TREF calibration procedure is based on the method proposed by Bonner et al. [18].

DSC was used to investigate the melting properties of nascent polymer samples. A TA Instrument Model DSC2910 was used for the measurements; endotherms of nascent polymers were obtained by scanning from an initial temperature of 0 °C to a final temperature of 160 °C at a rate of 10 °C/min. Calibration of the instrument was done with an indium standard. Repeat scans were done for each sample, but the first scans of the nascent polymers were of special interest since they provided information on the crystalline domains of the polymer as formed in the reactor.

Molar mass distributions of the PE products were measured with an Alliance GPCV2000 size exclusion chromatograph equipped with three Waters HTGE columns. HPLC grade 1,2,4-trichlorobenzene, obtained from Fisher Scientific to which was added 0.25 g/l of 2,6,-tert-butyl-4-methylphenol as an antioxidant, was used as the solvent. The columns and detectors were operated at 145 °C and the solvent rate was 1.0 cm^3/min. Polystyrene standards, C_{20}, C_{40} and C_{60} linear alkanes, and polyethylene reference materials 1475, 1482, 1483 and 1484 (from NIST) were used as standards for molar mass calibrations. Repeat analyses were done on all samples; the reported values are linear polyethylene equivalent molar masses.

Surface area and pore size distribution of the support for CAT2.5 were measured in the same manner as previously described for the other supports [7]. That is, an Omnisorp 360 was used to measure nitrogen uptakes, at liquid nitrogen temperature, and the BET method was used to calculate the surface area and the BJH equation was used to calculate the pore size distribution.

3. Results and discussion

3.1. Catalytic activity

Recently, Kumkaew et al. [7] showed that the pore size of mesoporous molecular sieves used for preparing (*n*-BuCp)$_2$$ZrCl_2$–MAO/mesoporous molecular sieve catalyst had a significant effect on the activity of the catalysts. The most active catalyst had pore sizes of about 2–6 nm. The effect of temperature and 1-hexene concentration on copolymerization activity were not included in the previous study. Additional polymerization experiments were carried out with the new small-pore catalyst, CAT2.5; conditions used for these runs are described in Table 2. The 1-hexene partial pressure was significantly less than the 1-hexene vapor pressure for all runs except Run 9 for which the initial partial pressure of 1-hexene was only slightly less than its vapor pressure. The vapor pressure of 1-hexene was calculated using the Antoine equation and the constants in Poling et al. [19].

The effect of 1-hexene concentration on the activity and temperature profiles are shown in Fig. 1. The amount of 1-hexene had a large effect on the rate profile and the total yield. For initial 1-hexene concentrations of <12 mol/m^3 (Runs 2 and 3) the polymer yields were higher than the homopolymer yield (Run 1); for initial 1-hexene concentrations >18 mol/m^3, the yields (Runs 4–8) were lower than the homopolymer yield. The influence of the presence of comonomer on polymerization rates is complex and probably involves chemical effects, e.g. changes in propagation rate constants, as well as physical changes to the catalyst, e.g. different fragmentation, and changes to the structure of the polymer, i.e. changes in polymer

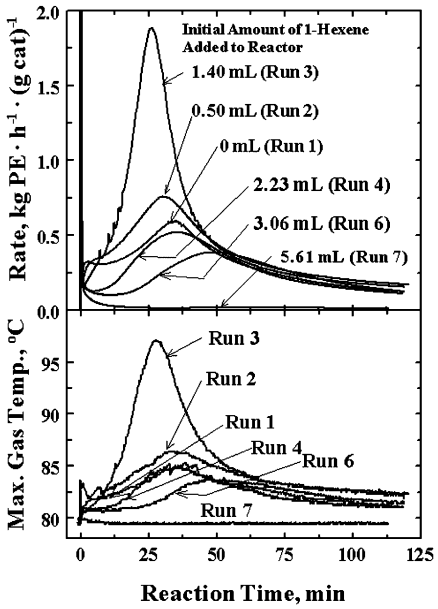

Fig. 1. Effect of 1-hexene concentration on rate and temperature profiles (CAT2.5).

Table 2
Description of polymerization runs

Run	Catalyst		Initial amount 1-C_6H_{12} (ml)	Initial temp. (°C)	Total pressure (MPa)	Total PE yield (g)	Run length (h)
	Type	Amount (mg)					
1	CAT2.5	50.5	0	80	1.34	28.3	1.97
2	CAT2.5	51.2	0.50	80	1.34	35.7	2.01
3	CAT2.5	50.6	1.40	80	1.35	51.5	1.98
4	CAT2.5	50.8	2.23	80	1.34	24.5	1.90
5	CAT2.5	48.0	2.20	80	1.35	12.6	1.93
6	CAT2.5	49.9	3.06	80	1.34	22.6	1.98
7	CAT2.5	50.1	5.61	80	1.35	3.1	1.88
8	CAT2.5	51.0	5.03	80	1.41	2.4	1.93
9	CAT2.5	46.2	2.24	40	1.37	2.2	1.95
10	CAT2.5	48.1	2.22	60	1.41	3.1	1.96
11	CAT2.5	47.6	2.21	90	1.37	18.0	1.97
12	CAT2.5	45.5	2.20	100	1.37	5.6	1.90
13	CAT20	51.1	3.40	70	1.37	6.5	2.00
14	CAT20	49.6	3.46	70	1.37	3.3	1.02
15	CAT20	53.5	3.47	70	1.38	0.7	0.51
16	CAT0.54	50.2	3.30	70	1.38	5.7	2.01
17	CAT2.6	51.6	3.23	70	1.38	34.3	2.05
18	CAT5.8	50.8	3.30	70	1.37	14.4	2.09
19	CAT7.2	50.1	3.43	70	1.37	3.4	2.00
20	CAT15	49.1	3.38	70	1.38	0.6	2.00

crystallinity [20]. The investigation of the comonomer effect was not the objective of the current study, but the observations on the effects of initial 1-hexene concentration on gas-phase polymerization rates may be of interest because most of the investigations into the comonomer effect have been done in slurries. The presence of 1-hexene resulted in a sharp decrease in initial rates compared to the initial homopolymerization rate; the sharp initial decrease was followed by a slower increase in the rate (see Fig. 1). These observations with 1-hexene are similar to those reported by Wester and Ystenes [20]. The rate at which rates increased in our gas-phase studies was a very strong function of the 1-hexene concentration; at low initial concentrations (<12 mol/m^3) the rates increased rapidly and exceed the homopolymerization rates after a few minutes. At higher initial 1-hexene concentrations the rate increases were much slower. For Run 7, the highest 1-hexene concentration (47 mol/m^3), the rate did not increase at all and remained very low for the duration of the 2 h run; a repeat experiment (Run 8) confirmed the low rates observed for Run 7.

Wester and Ystenes [20] ascribe the increase in the rate due to the comonomer to an increase in the fracturing rate of the catalyst. Improved fracturing in the presence of 1-hexene probably contributed to the rate increase, but it is difficult to explain the great sensitivity to 1-hexene concentration solely to a physical effect such as fracturing. Mass transfer effects cannot be used to explain the behavior because mass transfer limitation are very unlikely at the relatively low polymerization rates (<2 kg PE/(g cat·h) of this study [21,22]. The increased ethylene solubility in the more amorphous product made in the presence of 1-hexene is small and cannot be a significant factor in the observed effect of 1-hexene on the ethylene polymerization rate.

However, heat transfer effects did influence to rate profiles. The rapid increases in the polymerization rate at the low 1-hexene concentrations were accompanied by significant increases in the gas-phase temperatures (see bottom panel of Fig. 1). The increases in the temperature resulted in additional increases in rate, but the conclusion that small amounts of 1-hexene resulted in large increases in rate is valid even if Runs 2 and 3 were not isothermal because the increase in the temperature is the result of the increased rate caused by the presence of 1-hexene. (Note: problems with temperature control during gas-phase polymerizations were recognized early in gas-phase polymerization studies with metallocene catalysts [23]).

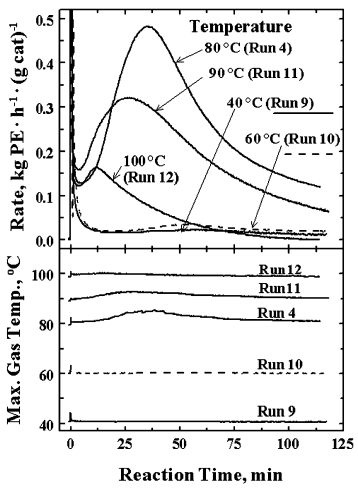

Fig. 2. Effect of reaction temperature on rate profiles (CAT2.5).

The effect of gas-phase temperature on copolymerization rates is shown in Fig. 2. These runs were done with an initial 1-hexene concentration of 18.7 (±0.2) mol/m^3; the maximum rates at this 1-hexene content were such that the increases in gas-phase temperature were small. Only for Run 4 was there an appreciable temperature increase and this was ≤5 °C; the temperature rise for all the other runs in this temperature series was ≤2 °C (see bottom panel of Fig. 2). Total polymer yields were very low for polymerization temperatures of 40 and 60 °C; repeat runs at these temperatures confirmed the low yields at 40 and 60 °C. Yields were maximum at 80 °C and then decreased with increasing temperature. Previously presented results for a similar catalyst, CAT2.6, showed that the copolymerization activity was also high at 70 °C [7]. The results show that the activation and deactivation rates of CAT2.5 are very temperature sensitive. The polymerization rates after 2 h of polymerization at 80, 90 and 100 °C were 0.12, 0.07 and 0.00 kg PE/(h·g cat), respectively. All the activity profiles shown in Fig. 2 have a maximum, and the reaction time required to reach this maximum increased with decreasing temperature, e.g. at 100 °C the rate maximum occurred after 11 min while 62 min were required at 40 °C. Average product yields for 2 h polymerization times increased by a factor of 8 for a temperature increase from 60 to 80 °C, and the maximum rates of polymerization for this temperature change increased by a factor of 14. The above results show that high gas-phase polymerization rates for the mesoporous silica supported (n-BuCp)$_2$ZrCl$_2$ catalyst resulted for narrow ranges of temperature (80–90 °C) and 1-hexene concentration (about 5–20 mol/m^3); much lower rates were observed outside of theses ranges.

Soga et al. [3] and Estrada and Hamielec [4] observed that properties of polyethylene produced in the slurry phase with homogenous metallocene catalysts were a function of reaction time. Three runs (Runs 13–15) were done to determine whether similar reaction-time dependent properties are obtained with a supported (n-BuCp)$_2$ZrCl$_2$ catalyst during gas-phase polymerization. CAT20 was used for these runs and the duration of these runs was 2.0, 1.0 and 0.5 h (other conditions are given in Table 2). The activity and temperature profiles are shown in Fig. 3, and the properties of the products produced are discussed in the sections below.

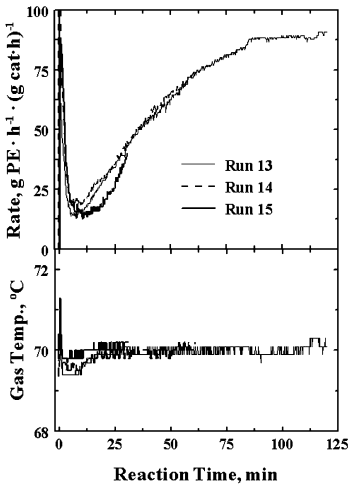

Fig. 3. Rate and temperature profiles for runs of different duration (CAT20).

The reproducibility of activity profiles during the first 30 and 60 min for the three runs shown in Fig. 3 was very good.

3.2. Characterization by temperature rising elution fractionation

TREF provides information on the structure of the polyethylene molecules (short chain branching distribution or methylene sequence distribution); it does not provide information on the morphology of the nascent polymer because the nascent structure is destroyed during the dissolution of the polymer. Analytical TREF analyses were done on all the samples for which DSC results were reported and the TREF results are summarized in Table 4. The average concentration of short chain branches, C_N expressed as CH_3 groups per 1000 carbon atoms, was obtained from the TREF profiles, like those shown in Fig. 4, by Eq. (2),

$$C_N = \frac{\int_{t_o}^{t_f} (IR)_{signal}[CH_3]_t dt}{\int_{t_o}^{t_f} (IR)_{signal} dt} = \frac{\int_{T_o}^{T_f} (IR)_{signal}[CH_3]_T dT}{\int_{T_o}^{T_f} (IR)_{signal} dT} \quad (2)$$

where $[CH_3]_t$ and $[CH_3]_T$ are the concentrations of CH_3 groups per 1000 carbon atoms in the eluted polyethylene as a function of elution time and elution temperature, respectively, and $(IR)_{signal}$ is the time varying output of the IR cell during the TREF elution. Eq. (1) was used to calculate $[CH_3]_T$. The elution time and elution temperature can be interchanged in Eq. (2) because the temperature was a linear function of time. An estimate of the 'broadness' of the short chain branching contribution can be obtained from the C_W/C_N ratio [17]; C_W is defined by Eq. (3)

$$C_W = \frac{\int_{t_o}^{t_f} (IR)_{signal}[CH_3]_t^2 dt}{\int_{t_o}^{t_f} (IR)_{signal}[CH_3]_t dt} = \frac{\int_{T_o}^{T_f} (IR)_{signal}[CH_3]_T^2 dT}{\int_{T_o}^{T_f} (IR)_{signal}[CH_3]_T dT} \quad (3)$$

The fraction of homopolymer, F_{homo}, was taken as the fraction of polymer which eluted above 90.5 °C, i.e.

$$F_{homo} = \frac{\int_{90.5}^{T_f} (IR)_{signal}[CH_3]_T dT}{\int_{T_o}^{T_f} (IR)_{signal} dT} \quad (4)$$

An elution temperature of 90.5 °C, according to Eq. (1), corresponds to a concentration of 4 [CH_3] groups per 1000 carbons.

The fraction of the initially added 1-hexene which was consumed by polymerization, $F_{C6,reacted}$, was estimated from the average short chain branch content, C_N, and the amount of polymer produced, m_{PE}, by using Eq. (5)

$$F_{C6,reacted} = \frac{m_{C6,PE}}{m_{C6,0}} = \frac{0.006 m_{PE} C_N}{\rho_{C6} V_{C6,0}} \quad (5)$$

where $m_{C6,PE}$ is the amount of 1-hexene incorporated into the polymer; $m_{C6,0}$ is the mass of 1-hexene charged to the reactor; ρ_{C6} is the density of liquid 1-hexene (0.6731 g/cm^3) and $V_{C6,0}$ is the volume of 1-hexene fed to the reactor at the beginning of the run. The gas-phase 1-hexene concentration was measured by gas chromatography at the beginning and at the end of the run for Run 5. The measured 1-hexene concentration at the end of Run 5 was 6.4 mol/m^3, which corresponds to 0.50 g of 1-hexene in the gas phase (the final void volume of the reactor was about 935 cm^3 after subtracting the volumes of the product and the salt seedbed). The initial amount of 1-hexene charged to the reactor was 1.48 g (2.20 ml). Hence, 66% of the 1-hexene was removed from the gas phase; some of the 1-hexene was reacted and some was dissolved in the 12.6 g of product. According to the TREF analysis, 37% of the 1-hexene was removed due to reaction; this requires that 0.43 g of 1-hexene was dissolved in the 12.6 g of product, i.e. 0.034 g 1-hexene per gram of product. The solubility of 1-hexene in the product from Run 5 was estimated to be 0.02–0.04 g 1-hexene per gram of polyethylene from the results obtained by Moore [24,25]. The agreement between the 1-hexene consumption obtained by gas chromatography and that based on the TREF results is an indication that the short chain branching concentration measured is reliable.

Multiple peaks in TREF profiles are usually attributed to the presence of different types of catalytic sites [3,26]; the TREF profiles for Runs 13–15 in Fig. 4 all have two distinct peaks. This suggests that CAT20 has at least two different types of catalytic sites. The intensity of the high temperature peak at about 96 °C decreases with increasing reaction time; this PE eluted at 96 °C is essentially an ethylene homopolymer. Soga et al. [3] also observed that the fraction of highly crystalline PE decreased with increasing reaction time obtained for ethylene/1-hexene copolymerization in the slurry phase using a homogeneous Cp_2ZrCl_2–MAO catalyst. The change in the fraction of crystalline PE with increasing reaction time implies that the concentration of catalytic sites responsible for the formation of the crystalline PE decreases with time. This decrease can be due to the rapid deactivation of these sites or to the transformation of these sites to sites which incorporated 1-hexene more readily; such a transformation has been suggested by Estrada and Hamielec [4]. It should be pointed out that the 1-hexene concentration at the end of the 2-h run, Run 13, was less than the 1-hexene concentration at the end of the shorter runs; nevertheless, the fraction of homopolymer formed decreased with increasing reaction time (Table 3). Mass transfer limitations are extremely unlikely at the low rates obtained with CAT20, but even if mass transfer limitations were present, they cannot be responsible for the decreased homopolymer formation with increasing reaction time, because mass transfer limitations for gas-phase polymerizations result in an accumulation of the least reactive monomer in the interior of the polymer/catalyst particle due to convective mass transfer [22]. Hence, mass transfer limitations, which are more pronounced in the initial stages of polymerization, would result in an increase in 1-hexene incorporation during the early stages of polymerization; this is contrary to the observed effect.

The pore size of the supports had a significant effect on

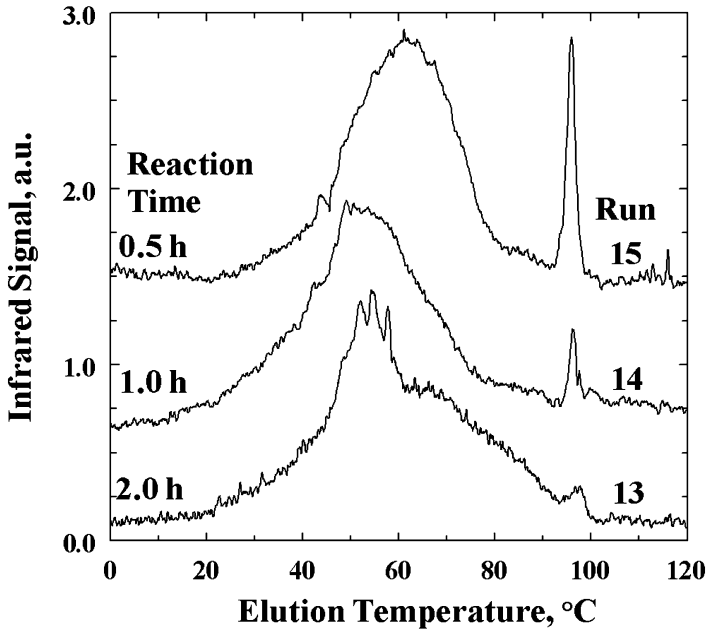

Fig. 4. Effect of reaction time on TREF profiles (CAT 20; patterns offset for clarity).

Table 3
Summary of TREF results

Run	Average CH_3 concentrations, CH_3 groups/1000 C		C_W/C_N	Fraction homo-polymer	Fraction 1-hexene reacted	1-Hexene concentrations (mol/m^3)	
	C_N	C_W				Initial	Final
1	0.5	0.5	1.02	0.99	–	0	0
2	3.1	9.3	2.98	0.88	1.00	4.2	0
3	2.9	4.2	1.44	0.80	0.96	11.8	0.5
4	5.7	8.8	1.55	0.47	0.56	18.8	8.3
5	7.3	9.3	1.28	0.09	0.37	18.5	11.7
6	9.0	11.9	1.32	0.07	0.59	25.8	10.6
7	23.2	27.1	1.17	0.00	0.11	47.2	42.0
8	24.1	27.0	1.12	0.00	0.09	42.3	38.5
9	28.7	35.8	1.25	0.05	0.25	18.9	14.2
10	13.7	16.6	1.21	0.05	0.17	18.6	15.2
11	7.5	9.0	1.20	0.05	0.55	18.6	8.3
12	8.6	9.8	1.14	0.02	0.19	18.5	15.0
13	22.3	28.5	1.28	0.03	0.38	28.6	17.7
14	23.7	28.3	1.19	0.05	0.20	29.1	23.3
15	18.0	21.0	1.17	0.09	0.03	29.2	28.3
16	24.8	29.1	1.17	0	0.38	27.8	17.2
17	9.1	16.1	1.77	0.34	0.86	27.2	3.8
18	12.5	21.4	1.71	0.16	0.48	27.8	14.5
19	16.4	22.2	1.35	0.16	0.14	28.9	24.9
20	20.6	25.8	1.26	0.08	0.03	28.4	27.5

the short chain branching distribution of the products made with the different catalysts; the TREF profiles of LLDPE made at similar reaction conditions, with catalysts of different pore size, are shown in Fig. 5. All the TREF profiles in Fig. 5, except the one for CAT0.54, have two or more distinct maxima; again indicating multiple types of catalytic sites. An interesting feature of the TREF profiles in Fig. 5 is the systematic variation in their shape for increases in the support pore diameter from 2.6 to 20 nm. The TREF profile for CAT0.54 (Run 16) does not seem to fit the trend; CAT0.54 appears to behave as if it had large pores. This is reasonable because no reaction occurred inside the pores of this catalyst. We have previously shown that all the catalytic active species were on the outer surface [7]; hence, this catalyst can be considered to have pores of infinite size. The silicalite crystals did not fracture, but particles in all other catalyst fractured extensively, even the low activity CAT20. Previously, we suspected, based on scanning electron micrographs, that some parts of CAT20 may not have fractured [7]. However, subsequent EDX analysis of the areas we suspected to be unfractured catalyst particles revealed that they were sub-micron sized NaCl particles from the seedbed.

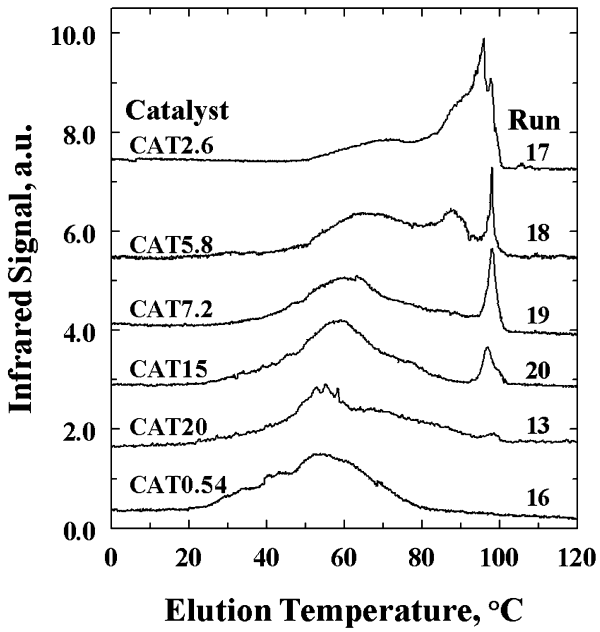

Fig. 5. Effect of support pore size on TREF profiles (patterns offset for clarity).

Two distinct peaks, one in the temperature range of 55–70 °C and the other at about 98 °C, are present in the TREF profiles. The low temperature peak is dominant in the large pore catalysts while the high temperature peak is more pronounced for the small pore catalysts. A third peak at about 88 °C is clearly visible in the profile for CAT5.8 (two repeat TREF analyses for this sample showed the same three peaks). This peak is also visible as a shoulder in the profile for CAT2.6. The presence of three distinct TREF peaks suggests that at least three different types of catalytic sites are present in these catalysts. The catalytic site corresponding to the peak at 98 °C produced ethylene homopolymer while the other two sites had differing 1-hexene incorporation rates. The results, discussed above, for the runs of

varying lengths (Runs 13–15) showed that the homopolymerization sites were also present in significant amounts at short polymerization times for the large-pored CAT20. However, the homopolymerization sites disappeared within the first two hours of polymerization for CAT20. The homopolymer content of products decreased with increasing pore size of the catalysts (Table 3; Runs 13, 17–20). From these observations, it is concluded that the nature of catalytic sites made during the impregnation of the supports with MAO and $(n\text{-BuCp})_2ZrCl_2$ is affected by the support pore size. The effect of the spatial constraint of small pores on the structure of MAO entering these pores is the most probable reason for the effect of pore size on the nature of the catalytic sites. The results of Sano and coworkers [8–11] clearly showed that segregation of MAO into different types of MAO molecules occurred when mesoporous silicas were placed in a MAO/toluene solution. The equilibrium distribution of MAO molecular structures may also be altered by the partitioning of different MAO molecules between the toluene solution and the volume in the pores. Fewer than 10 MAO molecules with a molar mass of 1000 [11] can be stacked across a 6 nm pore; $(n\text{-BuCp})_2ZrCl_2$, which is also a bulky molecule, will also be affected by the confines of the narrow pores. Hence, the size of the pore can affect the structure of MAO and the nature of the MAO-$(n\text{-BuCp})_2ZrCl_2$ interactions. Such different environments for different pore sizes can result in different catalytic behavior because, according to Lanz et al. [27], the 'cocatalysts-counterion *fit* and solvation play a significant role in the structures and energetics of the ion pairing, hence, catalytic activities and selectivities'. These effects will become less pronounced with increasing pore sizes.

A new catalyst with small pores, CAT2.5, was prepared to determine the effect of 1-hexene concentration and temperature on catalytic behavior and product properties. The TREF profiles of products made with CAT2.5 at 80 °C and different 1-hexene concentration are shown in Fig. 6. These profiles again show two main peaks; the high temperature peak being the dominant peak at low 1-hexene concentration and the low temperature peak being dominant at high 1-hexene concentrations. The shoulder on the high temperature peak becomes more prominent with increasing 1-hexene concentrations (Runs 2–4). At intermediate 1-hexene concentrations (Runs 5 and 6), the peak at 90 °C is dominant, and at high 1-hexene concentration only the low temperature peak is present. These results suggest that the activation of the catalytic sites is affected by the 1-hexene concentration; homopolymerization sites do not appear to be present at high 1-hexene concentrations. It is possible that 1-hexene participates in the conversion of homopolymerization sites to copolymerization sites.

Temperature also affects the short chain branching distribution; Fig. 7 shows the TREF profiles of products made with CAT2.5 at different temperatures with similar initial 1-hexene concentrations. The TREF profiles for products made at reaction temperatures of 40 and 60 °C (Runs 9 and 10) indicate that these materials were mainly copolymer; the shape of the profiles were similar to those obtained at high 1-hexene concentrations at 80 °C (Fig. 6). This is reasonable since the solubility of 1-hexene increases significantly with decreasing temperature. Increasing reaction temperature from 80 to 90 and 100 °C resulted in small increases in 1-hexene incorporation, but the yield of product at 100 °C was less than the yield at 80 and 90 °C.

The broadness of the short chain branching distribution is due to the presence of different types of catalytic sites as well as to variations in the 1-hexene concentration during the runs; the C_W/C_N values in Table 3 are an indication of the broadness of the short chain branching distribution. The TREF results showed that reaction time, support pore size, 1-hexene concentration and reaction temperature all significantly influenced the short chain branching distribution of the LLDPE made with $(n\text{-BuCp})_2ZrCl_2$ supported on MAO-treated mesoporous silicas. The TREF results also indicate that different types of catalytic sites are present in these catalysts and that the pore size influences the type of sites present.

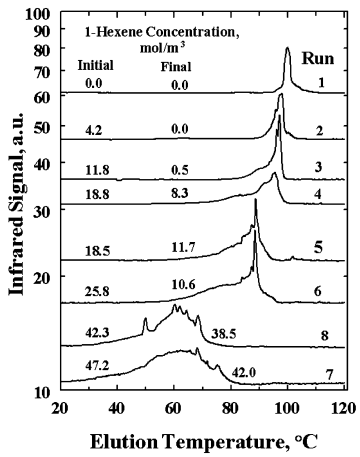

Fig. 6. Effect of initial 1-hexene concentration on TREF profiles (CAT2.5; note logarithmic ordinate; patterns offset for clarity).

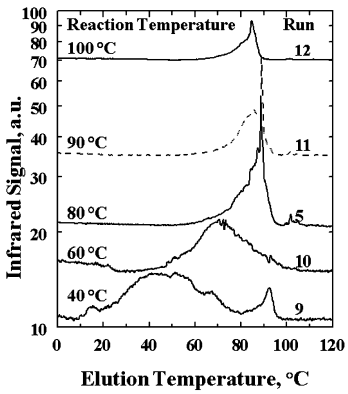

Fig. 7. Effect of reaction temperature on TREF profiles (CAT2.5; note logarithmic ordinate; patterns offset for clarity).

3.3. Characterization by differential scanning calorimetry

Information about the morphology can be obtained by DSC, i.e. variations in melting indicate the presence of crystalline lamellae with different thicknesses [28]. Two consecutive DSC scans were done on each sample to determine whether the DSC features of the nascent and recrystallized product were a function of the type of catalyst and the polymerization conditions. The first scan consisted of heating the nascent polymer in the calorimeter from 0 to 160 °C at a rate of 10 °C/min, followed immediately by cooling to 0 °C at the same rate. The second complete scan on the melt-recrystallized sample was done immediately after the first scan at the same heating rates. Fig. 8 shows the endotherms and exotherms for the two scans for the product from Run 18. The scans in Fig. 8 show that the endotherms for the nascent and melt-recrystallized polymers have several maxima indicating that crystalline lamellae with different thicknesses were present in the nascent and recrystallized product. This could be an indication of different types of catalytic sites. The endotherm for the second scan shows that melting and solidification of the first scan removes some of the complex structure of the endotherm, but in this, as well as many other samples, both endotherms had more than one peak, indicating multiple types of catalytic sites.

DSC endotherms for the runs with different lengths of polymerization are shown in Fig. 9 (Runs 13–15; CAT20). The similarity of the three endotherms for the nascent polymers (Fig. 9(a)) is striking; this reproducibility of the complex structure of the endotherm for the nascent polymers shows that the maxima in the endotherms are not the result of random events but are related to the nature of the catalyst and polymerization conditions; much of this detail is lost in the endotherms for the second scans (Fig. 9(b)) but all the endotherms for the second scan still had two

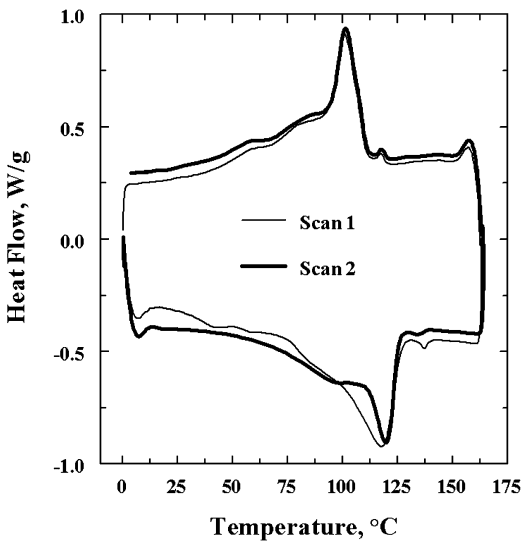

Fig. 8. Illustration of DSC endotherms and exotherms for two complete scans (Run 18).

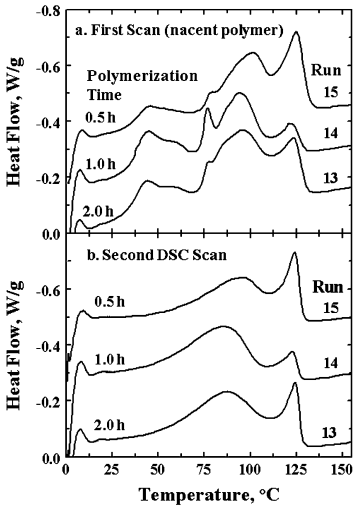

Fig. 9. Effect of reaction time on DSC endotherms for Scans 1 and 2 (CAT20).

well defined peaks. A short polymerization time (0.5 h; Run 15) resulted in endotherms in which the main peak is at high temperature (i.e. large lamellae). The main peak for Run 15 is at 125 °C while the main peaks for products made with longer polymerization time are at about 90 °C in the second scan. The observation that the amount of low crystallinity polymer, i.e. decrease in melting temperature, increases with increasing polymerization time is in agreement with the TREF profiles discussed above and the observations by Soga et al. [3].

The DSC endotherms for nascent polymers made at similar polymerization conditions (Run 13 and 16–20) with catalysts having different initial pore sizes are shown in Fig. 10. It is clear that the initial pore size has a marked effect on the nascent product morphology. Products made with catalysts with support pore sizes >7 nm (Runs 13, 19 and 20) had DSC endotherms with several maxima, in both first and second scans, indicating multiple types of catalytic

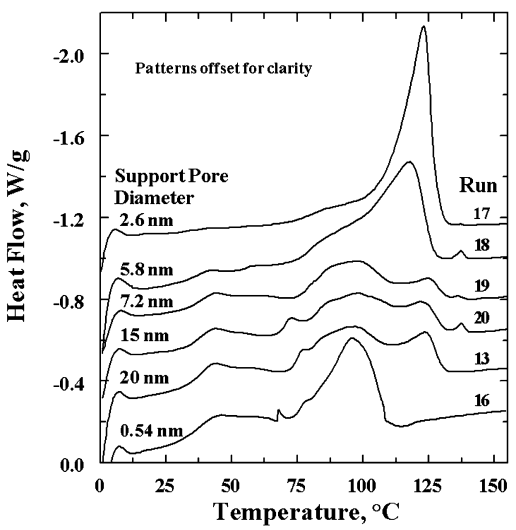

Fig. 10. Effect of pore size on DSC endotherms.

sites. Products made with CAT2.6 and CAT5.8 had simpler endotherms (Runs 17 and 18); the nascent product made with CAT2.6 only has one major peak in its endotherm. This indicates that catalytic sites in catalysts with initial pore size in the 2–6 nm range are not as varied as the catalytic sites in catalysts with larger initial pore sizes. Just as with the TREF results, the product made with the silicalite support (CAT0.54; Run 16) did not follow this above trend of greater product homogeneity with decreasing support pore size because the $(n\text{-BuCp})_2ZrCl_2$ did not enter the 0.54 nm pores of the support particles [7]. The main peak in the endotherms for the large pore catalysts (Runs 13, 19 and 20) and for CAT0.54 (Run 16) is at 96 °C, while the main peaks for the small pore size catalysts (Runs 17 and 18) are at about 120 °C. (Temperatures of maxima in the endotherms are listed in Table 4). The very systematic variation in the shapes of endotherms for nascent product as a function of initial catalyst pore size shows that the DSC endotherms of nascent polymer provides useful information about the catalytic polymerization process.

DSC endotherms of products made with CAT2.5 at various 1-hexene concentrations are shown in Fig. 11. Increases in the initial concentration of 1-hexene resulted in a systematic decrease in the temperature of the main peak in the endotherm as well as in the crystallinity based on the integrated heat of melting (Table 4; Runs 1–8). For initial 1-hexene concentrations ≤ 25 mol/m^3 (Runs 1–6), the endotherm was dominated by a single peak with a peak temperature which decreased from 139 to 119 °C with increasing 1-hexene concentration. A secondary peak, of

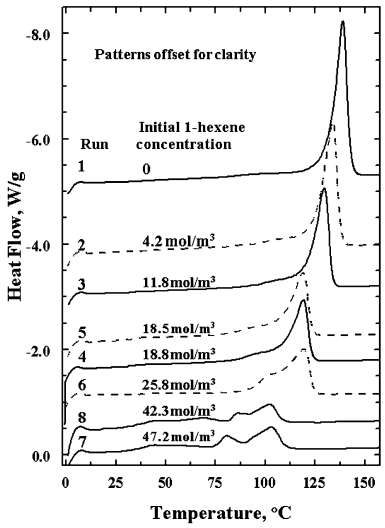

Fig. 11. Effect of initial 1-hexene concentration on DSC endotherms.

increasing intensity with increasing 1-hexene concentration, started to appear for these runs at about 105–95 °C. For initial 1-hexene concentrations >40 mol/m^3 (Runs 7 and 8), the high temperature peak at ≥ 119 °C disappeared and the peak at about 100 °C became the dominant peak. The marked change in the shapes of the DSC endotherms for the change in initial 1-hexene concentration from 26 to 42 mol/m^3 suggests that different types of catalytic sites interact differently with 1-hexene. These results are in general agreement with the TREF results. Changes in reaction temperature, at the same initial 1-hexene concentration, also results in products with different DSC endotherms. The

Table 4
Summary of DSC results

Run	Initial Temp. (°C)	Range of 1-C_6H_{12} concentr. (mol/m^3)	Catalyst	Maxima in DSC endotherms[a] (°C)					Crystallinity[b] (%)	
				T_1	T_2	T_3	T_4	T_5	Scan 1	Scan 2
1	80	0.0	CAT2.5	–	–	–	–	139*	56	58
2	80	4.2–0.0	CAT2.5	–	–	–	–	134*	55	54
3	80	11.8–0.5	CAT2.5	–	–	105	–	129*	46	46
4	80	18.8–8.3	CAT2.5	–	–	95	119*	–	42	40
5	80	18.5–11.7	CAT2.5	–	–	95	119*	–	41	38
6	80	25.8–10.6	CAT2.5	–	–	101	119*	–	35	35
7	80	47.2–42.0	CAT2.5	45	81	103*	–	–	26	20
8	80	42.3–38.5	CAT2.5	45	86	102*	–	–	27	19
9	40	18.9–14.2	CAT2.5	41	82*	100	118*	–	27	15
10	60	18.6–15.2	CAT2.5	42	89	–	112*	–	33	25
11	90	18.6–8.3	CAT2.5	–	80	–	120*	–	36	33
12	100	18.5–15.0	CAT2.5	–	77	–	117*	–	34	32
13	70	28.6–17.7	CAT20	44	78	96*	124	–	30	21
14	70	29.1–23.3	CAT20	45	77	94*	122	–	24	17
15	70	29.2–28.3	CAT20	45	78	101	125*	–	25	17
16	70	27.8–17.2	CAT0.54	46	78	96*	–	–	27	22
17	70	27.2–3.8	CAT2.6	–	–	88	123*	–	35	38
18	70	27.8–14.5	CAT5.8	43	–	88	118*	137	34	29
19	70	28.9–24.9	CAT7.2	44	–	96*	125	136	21	14
20	70	28.4–27.5	CAT15	44	73	97*	123	137	26	16

[a] The main DSC peak in the endotherm is indicated by an asterisk (*).
[b] DSC crystallinity based on $\Delta H_{fusion} = 290$ J/g for crystalline polyethylene [29].

DSC results on the effect of temperature were also in general agreement with the TREF results shown in Fig. 7.

The crystallinities calculated from the enthalpy of melting show an interesting trend (last 2 columns of Table 4). The crystallinities from Scan 1 and Scan 2 were approximately equal for all the relatively narrow endotherms which had one or two peaks, while the crystallinities based on DSC Scan 2 were considerably lower than the crystallinities based on Scan 1 for all the broad endotherms which had more than two peaks. The lower crystallinity for Scan 2 for the broad endotherms is due to the disappearance of the low temperature peak in Scan 2 (endotherms for Scans 1 and 2 in Fig. 9).

TREF and DSC studies indicate the heterogeneous nature of the catalytic sites in the supported $(n\text{-BuCp})_2ZrCl_2$ catalysts. DSC results generally indicate a greater degree of heterogeneity in catalytic sites as a function of pore size than the TREF results (Figs. 5 and 10), 1-hexene concentration (Figs. 6 and 11) and reaction temperature (Figs. 7 and 12). Only for the low 1-hexene concentration experiments with CAT2.5 were the DSC profiles less complex than the TREF profiles (Figs. 6 and 11). The morphology of the nascent polymers may also have been affected by the rate and degree of catalyst fracturing; some of the complex structures in the nascent DSC endotherms may be related to the fracturing process since this could effect the crystallization of the nascent polymer. Additional DSC characterization using thermally fractionated samples as well as TREF–DSC cross-fractionation studies may reconcile these differences.

3.4. Molar mass

We have previously reported that support pore size does not have a significant effect on molar masses for ethylene/1-hexene copolymers made at 70 °C with mesoporous silica-supported $(n\text{-BuCp})_2ZrCl_2$ catalysts [7]. The effect of 1-hexene concentration on molar masses of PE made with CAT2.5 at 80 °C is shown in Fig. 12. In Fig. 12, the molar masses are plotted as a function of the 'average' 1-hexene concentration; the average 1-hexene concentration is taken as the arithmetic average of the initial and final 1-hexene concentration (Table 3). A similar plot is obtained for molar masses as a function of initial 1-hexene concentration. As expected, the number average molar mass, M_N, decreases with increasing 1-hexene concentration. The mass average molar mass, M_W, is relatively unaffected by increases in 1-hexene concentration; this results in an increase in polydispersity from about 2.5 at low 1-hexene concentrations to a value of 4.0 at an average 1-hexene concentration of 45 mol/m^3.

The effect of temperature on molar masses of PE made with CAT2.5 at 80 °C and an initial 1-hexene concentration of 18.7 ($\pm$0.2) mol/m^3 is shown in Fig. 13. The molar masses are plotted as a function of reciprocal temperature and the equations describing the molar masses are:

$$\ln[M_N] = 7.946 + \frac{997}{T} \qquad \text{with } T \text{ in K} \tag{6}$$

and

$$\ln[M_W] = 8.306 + \frac{1197}{T} \qquad \text{with } T \text{ in K} \tag{7}$$

The decrease in molar masses with increasing temperature shows that the activation energies for chain termination are larger than those for propagation; based on Eq. (6), the lumped activation energy for termination exceeds the lumped activation energy for propagation by about 8.3 kJ/mol. The relatively good correlation of M_N with $1/T$, even

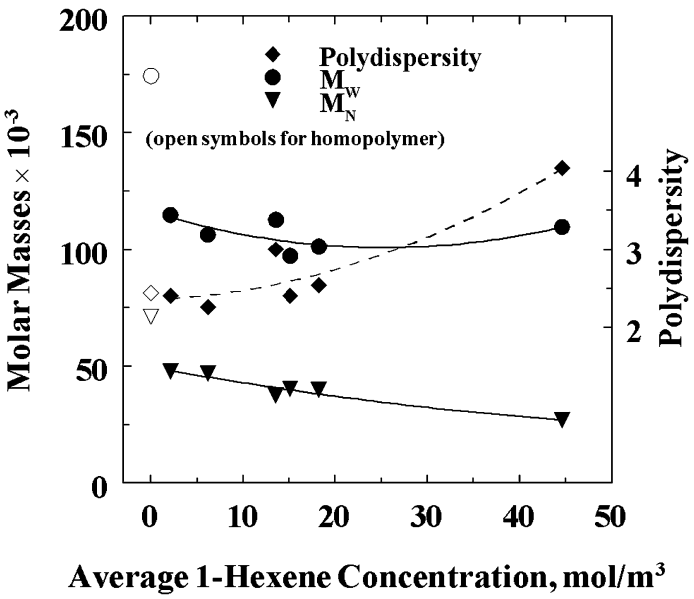

Fig. 12. Effect of 1-hexene concentration on molar mass and polydispersity (CAT2.5; Runs 1 to 7).

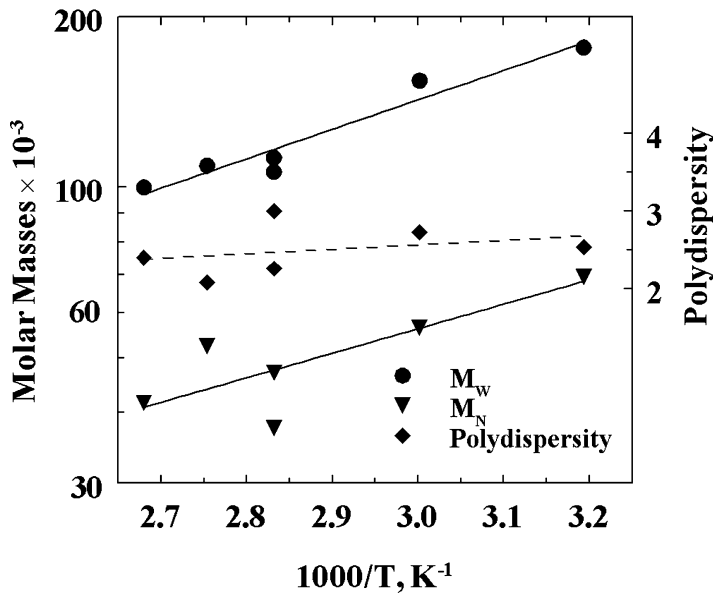

Fig. 13. Effect of reaction temperature on molar mass and polydispersity (CAT2.5; Runs 4, 5, and 9–12).

though the properties of products as indicated by TREF and DSC varied significantly with temperature, suggests that the temperature dependencies of the propagation and termination reactions are not significantly affected by the changes in 1-hexene incorporation rates.

4. Summary and conclusions

Gas-phase ethylene polymerization rates as well as 1-hexene incorporation rates over $(n\text{-BuCp})_2ZrCl_2$ supported on MAO-treated mesoporous molecular sieves are a strong function of the pore size of the support. Catalysts with support pore size in the 2–6 nm range had the highest ethylene polymerization rates [7], and catalysts with larger pore size had higher 1-hexene incorporation rates. Ethylene polymerization rates were a strong function of 1-hexene concentration and temperature. For a small-pored catalyst (CAT2.5), the polymerization rate was highest at 80 °C. Low concentration of 1-hexene (4–12 mol/m^3) caused significant increases in ethylene polymerization rates compared to ethylene homopolymerization rate. The copolymerization rates were lower than the homopolymerization rate at 1-hexene concentrations above 20 mol/m^3. The variations in rate behavior with support pore size suggest that the pore size of the support affects the type and concentration of active sites.

TREF characterization of the products made with different pore size catalysts and different polymerization conditions confirmed that the mesoporous molecular sieve-supported $(n\text{-BuCp})_2ZrCl_2$ catalysts contained multiple types of catalytic sites and that the type and/or concentration of the various catalytic sites was dependent on the pore size of the support. TREF analysis of products obtained from experiments for different lengths of polymerization showed that the distribution of sites was time dependent; sites with no or low 1-hexene incorporation rates were more prevalent at short polymerization times. DSC results confirmed the TREF results. The DSC experiments with the nascent products showed that multi-peaked DSC endotherms were reproducible and were very dependent on catalyst and the polymerization conditions. This suggests that DSC of nascent polymer may provide information on heterogeneity of supported polymerization catalysts. The molar masses were not a strong function of support pore size [7] and the variation of molar masses with 1-hexene concentration and temperature followed the expected trends, i.e. decreases in molar masses with increasing 1-hexene concentration and increasing temperature.

Acknowledgements

The authors would like to acknowledge the support of this work by the Natural Sciences and Engineering Research Council of Canada (NSERC), and we thank the Thailand Research Fund (TRF) for their financial support. We also thank N. Bu for the molar mass measurements.

References

[1] Janiak C, Rieger B. Angewand Makromol Chem 1994;215:47–57.
[2] Galland GB, Seferin M, Mauler RS, Dos Santos JHZ. Polym Int 1999; 48:660–4.
[3] Soga K, Uozumi T, Arai T, Nakamura S. Macromol Rapid Commun 1995;16:379–85.
[4] Estrada JMV, Hamielec AE. Polymer 1994;35:808–18.
[5] Wang Q, Weng J, Xu L, Fan Z, Feng L. Polymer 1999;40:1863–70.
[6] Kim JD, Soares JBP. Macromol Rapid Commun 1999;20:347–50.

[7] Kumkaew P, Wanke SE, Praserthdam P, Danumah D, Kaliaguine S. J Appl Polym Sci 2003;87:1161–77.
[8] Sano T, Doi K, Hagimoto H, Wang Z, Uozumi T, Soga K. Chem Commun 1999;733–4.
[9] Sano T, Doi K, Hagimoto H, Wang Z, Uozumi T, Soga K. Stud Surf Sci Catal 1999;125:777–84.
[10] Sano T, Hagimoto H, Jin J, Oumi Y, Uozumi T, Soga K. Macromol Rapid Commun 2000;21:1191–5.
[11] Sano T, Hagimoto H, Sumiya S, Naito Y, Oumi Y, Uozumi T, Soga K. Microporous Macroporous Mater 2001;44:557–64.
[12] Lehmus P, Härkki O, Leino R, Luttikhedde HJG, Näsman JH, Seppälä JV. Macromol Chem Phys 1998;199:1965–72.
[13] Yoon JS, Lee DH, Park ES, Lee IM, Park DK, Jung SO. J Appl Polym Sci 2000;75:928–37.
[14] Foxley D. Chem Ind 1998;8:305–8.
[15] Lynch DT, Wanke SE. Can J Chem Eng 1991;69:332–9.
[16] Huang JCK, Lacombe Y, Lynch DT, Wanke SE. Ind Engng Chem Res 1997;36:1136–43.
[17] Zhang M, Lynch DT, Wanke SE. J Appl Polym Sci 2000;75:960–7.
[18] Bonner JG, Frye CJ, Capaccia G. Polymer 1993;34:3532–4.
[19] Poling BE, Prausnitz JM, O'Connell JP. The properties of gases and liquids, 5th ed. New York: McGraw Hill; 2001. p. 7.4 and A.53.
[20] Wester TS, Ystenes M. Macromol Chem Phys 1997;198:1623–48.
[21] McKenna TF, Cokljat D, Spitz R, Schweich D. Catal Today 1999;48: 101–8.
[22] Kittilsen P, Svendsen H, McKenna TF. Chem Engng Sci 2001;56: 3997–4005.
[23] Roos P, Meier GB, Samson JJC, Weickert G, Westerterp KR. Macromol Rapid Commun 1997;18:319–24.
[24] Moore SJ, Wanke SE. Chem Engng Sci 2001;56:4121–9.
[25] Moore SJ. Solubility of α-olefins in polyethylenes. MSc Thesis. Department of Chemical and Materials Engineering, Univ of Alberta; 2000.
[26] Soares JBP, Hamielec AE. Macromol Theor Simul 1995;4:305–24.
[27] Lanz G, Fragalà IL, Marks TJ. Organometallics 2002;21:5594–612.
[28] Zhou H, Wiles GL. Polymer 1997;38:5735–7.
[29] Ottani S, Porter RS. J Polym Sci: Part B, Polym Phys 1991;29: 1179–88.